Communications in Physics, Vol. 33, No. 1 (2023), pp. 103-110
DOI: https://doi.org/10.15625/0868-3166/17513

Design hetero-nanojunction of RGO/α-Fe_2O_3 nanofibers for ethanol gas sensor

Phan Hong Phuoc[1], **Le Viet Thong**[1,†], **Nguyen Van Hoang**[2], **Nguyen Duc Hoa**[3], **Nguyen Van Duy**[3], **Nguyen Ngoc Viet**[1] **and Nguyen Van Hieu**[1,4,‡]

[1]*Faculty of Electrical and Electronic Engineering, Phenikaa University, Hanoi, Vietnam*

[2]*Department of Materials Science and Engineering, Le Quy Don Technical University, Hanoi, Vietnam*

[3]*International Training Institute for Materials Science, Hanoi University of Science and Technology, Hanoi, Vietnam*

[4]*Phenikaa Research and Technology Institute (PRATI), A&A Green Phoenix Group, Hanoi, Vietnam*

E-mail: [†]thong.leviet@phenikaa-uni.edu.vn; [‡]hieu.nguyenvan@phenikaa-uni.edu.vn

Received 15 September 2022; *Accepted for publication 30 October 2022*
Published 21 February 2023

Abstract. *Enhanced gas sensing properties of hematite α-Fe_2O_3 by loaded reduced graphene oxides (RGO) have attracted considerable attention. In this study, RGO-loaded α-Fe_2O_3 nanofibers were fabricated via the facile electrospinning technique followed by a calcination process. The scanning electron microscopy (SEM) images presented RGO-loaded α-Fe_2O_3 nanofibers with diameters of 50-100 nm have typical spider nets-like morphologies. The X-ray diffraction (XRD) patterns manifested the rhombohedral structure of the RGO-loaded α-Fe_2O_3 nanofibers. The energy-dispersive X-ray spectroscopy (EDS) results exhibited the existence of Fe, O, and C elements in the synthesized nanofibers. The gas sensing results also confirmed that the sensors based on RGO-loaded α-Fe_2O_3 nanofibers could be applied for detecting ethanol gas.*

Keywords: RGO; electrospinning; RGO-loaded α-Fe_2O_3 nanofibers; ethanol.

Classification numbers: 07.07.Df; 81.05.ue; 81.16.Hc.

1. Introduction

Nanofibers (NFs) are 1D nanostructures that are increasingly used in gas sensor applications because of their unique properties such as porous structure and large specific surface area [1, 2]. Different approaches including self-assembly, template synthesis, drawing, phase separation and electrospinning have been reported for the fabrication of NFs [1,2]. Among them, electrospinning believed to be the most adaptable cheap technique to synthesize NFs. The NF produced by electrospinning has numerous remarkable advantages such as a high aspect ratio, and flexibility for chemical/physical functionalization [2]. Thus, this technique has been widely used to synthesize NFs for gas sensor applications [3].

Hematite (α-Fe_2O_3), a low-cost and non-toxic transition semiconductor metal oxide with a band gap of 2.2 eV, is one the most stable candidate in the iron oxide family under air conditions [4–6]. This material has gained increasing attention in the gas sensing field due to its ability to detect various gases such as NO_2, NH3, CO, H_2S, C3H7OH, C_2H_5OH, and CH3OH [5]. Recently, reduced graphene oxides (RGO), a type of graphene which is reduced from graphene oxides produced from graphite by the Hummer method [7], have received worldwide attention thanks to their exceptional physicochemical properties [8–10]. The combination between α-Fe_2O_3 and reduced graphene oxides (RGO) for gas sensor applications to enhance the gas sensing performance through the formation of heterojunction is mentioned in many works [11–15]. For instance, Guo *et al.* [11] reported that the response of 1 wt% RGO/α-Fe_2O_3 nanofiber to 100 ppm acetone at the working temperature of 375°C is about 8.9 (4.5 times higher than that of pure α-Fe_2O_3). Liang and his coworkers [12] used a hydrothermal method to produce a composite of RGO/α-Fe_2O_3 particles to enhance the ethanol gas sensing properties of α-Fe_2O_3. Hu *et al.* [13] used quantum dots/α-Fe_2O_3 composites to increase the gas-sensing response and the gas-sensing selectivity to TMA. H. Zhang *et al.* [14] also reported that the RGO/α-Fe_2O_3 nanocomposite-based sensor exhibited a high response of 3.86 to 5 ppm NO_2 at room temperature compared to pure RGO (1.38). B. Zhang and his coworkers [15] showed that the composite containing 1.0 wt% RGO exhibited an enhanced gas response of 13.9 to 100 ppm acetone at the operating temperature of 225°C, approximately 2.5-fold higher than that of pure α-Fe_2O_3 (5.5). It is obvious that the nanocomposite of RGO and α-Fe_2O_3 can significantly enhance the gas sensing properties. However, until now, research on the ethanol gas sensor based on RGO-loaded α-Fe_2O_3 NFs has not gained much success yet although Guo *et al.* [11] presented an enhanced response to ethanol of the sensor based on RGO-loaded α-Fe_2O_3 NFs in selectivity section.

In this study, the RGO-loaded α-Fe_2O_3 NFs were synthesized by the electrospinning method. Accordingly, the characterizations of as-prepared NFs were clearly analyzed. The ethanol gas sensing properties of the sensor based on RGO-loaded α-Fe_2O_3 NFs were investigated in detail.

2. Experiment

The reduced graphene oxides (RGO) were obtained followed by the Hummers method, in which the graphene oxides (GO) have been used as a source material [7]. As-synthesized RGO was dispersed in deionized water (DI) for further use. Analytical reagent Fe(NO3). 9H_2O and PVA were completely dissolved in DI under magnetic stirring for 2 h. Then, a suitable amount of RGO (the weight ratio of RGO/Fe_2O_3 was 1 wt%) was added into the above-mixed solution, followed by stirring for 22 h to obtain a homogeneous solution. RGO-loaded α-Fe_2O_3 NFs were fabricated by the electrospinning method, followed by aged at 600°C for 3 h in air, as reported in our previous works [16–18].

The phase structure of RGO-loaded α-Fe_2O_3 NFs was characterized by X-ray diffraction (XRD, Bruker D5005). The crystallize size was calculated by the Scherrer formula, $D = 0.9\lambda/(\beta\cos\theta)$, where λ was the X-ray wavelength, θ was the diffraction angle of the (104) planes of the as-synthesized NFs and β was the full width at haft maximum (FWHM) of the observed peak [17]. The morphologies of as-synthesized NFs were obtained by field emission scanning electron microscope (FESEM, Hitachi S-4800). The elemental compositions of NFs were examined by energy dispersive X-ray spectroscopy (EDX, attached in FESEM). Raman spectra were performed on a Raman spectrometer (LabRAM HR 800, Horiba-Jobin Yvon, France).

The gas sensing properties of the sensor based on RGO-loaded α-Fe_2O_3 NFs were measured by a flow-through technique [19–21]. The sensor response was defined as the ratio of the sensor resistance S = Ra/Rg where Ra and Rg were sensor resistances in dry air and tested gas, respectively. Response time (τ_{res}) and recovery time (τ_{rev}) were estimated when sensor resistance reached a 90% change of the initial value after exposing or removing tested gas.

3. Results and discussion

The morphologies of the RGO and RGO loaded- α-Fe_2O_3 NFs samples were shown in Fig. 1. As seen in Fig. 1a, the graphene nanosheets were prepared because of the harsh oxidation in Hummmer's process. In Fig. 1b, RGO loaded- α-Fe_2O_3 NFs with a diameter of about 50-100 nm were synthesized successfully by the electrospinning method. The rough surfaces' NFs noticed because the as-prepared NFs were composed of many nanograins. The insert of Fig.1b was a FESEM image at low magnification. The RGO loaded-α-Fe_2O_3 NFs presented the typical spider-net-like morphology of NF feature fabricated by electrospinning [18]. The NFs were uniform, continuous, and well-dispersed on the electrode substrate.

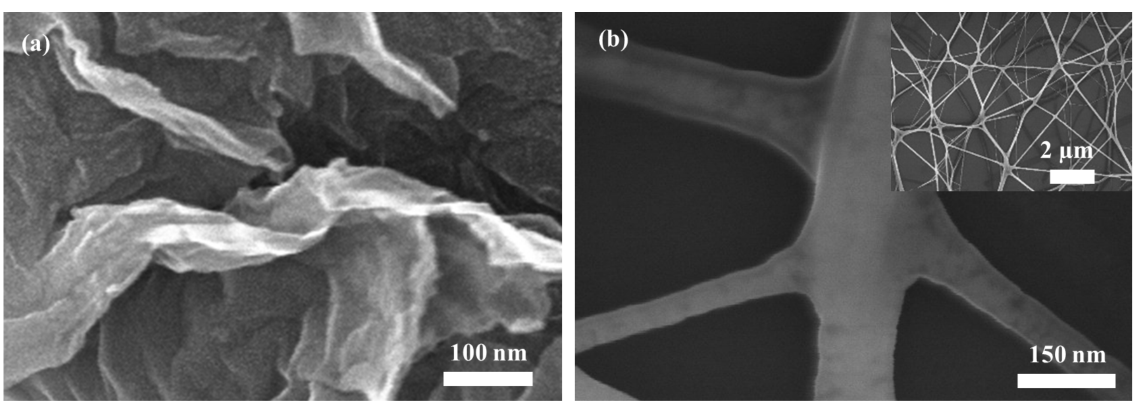

Fig. 1. FESEM images of as-synthesized RGO (a) and RGO loaded-α-Fe_2O_3 nanofibers (b).

The elemental composition, and crystal properties of the RGO loaded-α-Fe_2O_3 NFs were exhibited in Fig. 2. The as-spun fibers exhibited no diffraction peaks, this phenomenon explained by their amorphous nature, whereas, the calcined NFs were shown to have the peaks of (012),

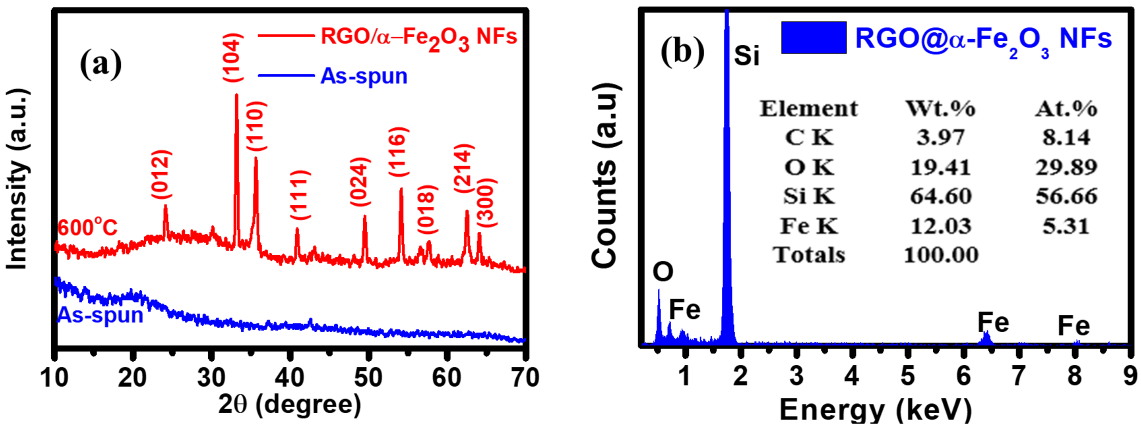

Fig. 2. XRD patterns (a) and EDX spectrum (b) of RGO loaded α-Fe_2O_3 NFs.

(104), (110), (111), (024), (116), (018), (214) and (300) agreeing well with the standard values of JCPDS ICDD card No. 33-0664 for the rhombohedral structure of hematite α-Fe_2O_3 (Fig. 2a). There were no typical diffraction peaks of RGO in the XRD results of the mixture between α-Fe_2O_3 and little content of RGO due to seriously broken and separated RGO nanosheets during the preparation process, which was reported in other literatures [14, 15]. The nanograin size of RGO-loaded α-Fe_2O_3 NFs calculated from the experimental XRD data was approximately 29 nm. The EDX spectrum in Fig. 2b showed the presence of Fe, O, and C elements from the RGO loaded-α-Fe_2O_3 NFs. Si element came from Si/SiO_2 electrode substrate. The amount of Fe, and C elements was quite small compared to that of Si element because the NFs dispersed across the substrate with a low density as shown in Fig. 1b.

The gas sensing properties of the sensor based RGO-loaded α-Fe_2O_3 NF sensors were presented in Fig. 3. The transient response curve of the sensor to various ethanol gas concentrations from 100 to 1000 ppm at different working temperatures of 300 – 400°C was presented in Fig. 3a. The sensor based on RGO loaded α-Fe_2O_3 NFs exhibited a typical sensing behavior of n-type semiconductor. When the sensor was introduced to reducing ethanol gas, the sensor resistance decreased and then recovered to initial values after being refreshed with dry air and the tested gas had been removed. The sensor response as a function of the ethanol gas concentrations at different working temperatures was also shown in Fig. 3b. The sensor response increased when the gas concentrations and working temperatures increased from 100 to 1000 ppm and 300 to 400°C, respectively. These results can be explained by the gas sensing mechanism of the sensor based on NFs as mentioned in our reported works [22–24]. In brief, when the NFs were exposed to the air, the NFs absorbed oxygen molecules to form negatively charged surface oxygen (O^-) by capturing free electrons from the conduction band of the NFs. Besides, the electron from RGO ($\Psi = 5.2$ eV) was transferred to α-Fe_2O_3 ($\Psi = 5.9$ eV) as a resulting of the difference in the work function [25, 26]. Thus the resistance of the sensor was significantly increased as a result of the RGO/α-Fe_2O_3 heterojunction formation. When C_2H_5OH gas was introduced to NFs, the reducing C_2H_5OH molecules interacted with the oxygens adsorbed in the following ways [12,24]:

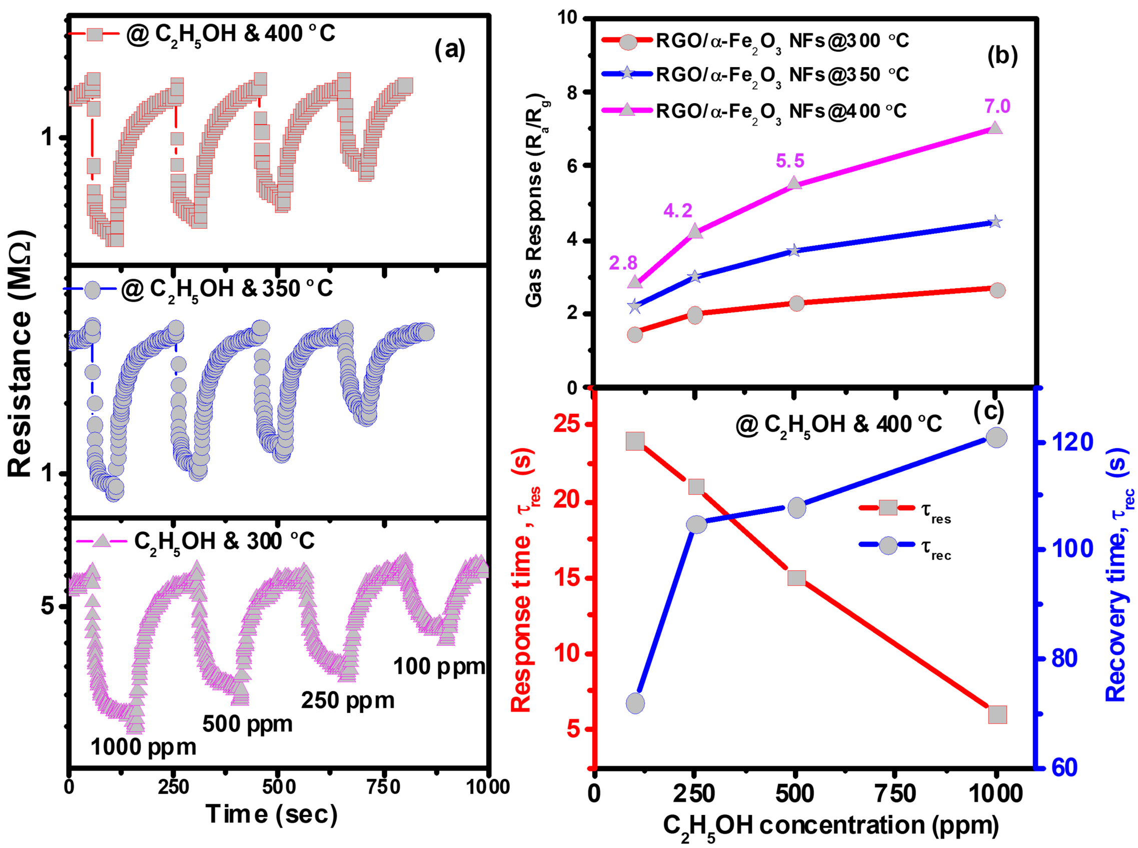

Fig. 3. Dynamic response (a), sensor response as a function of C_2H_5OH concentrations (b) at different working temperature and response-recovery time at the working temperature of 400˚C of the sensors based on RGO loaded α-Fe_2O_3 NFs.

$C_2H_5OH(gas) + 6O^-$ (ads) = $2CO_2(gas) + 3H_2O(gas) + 6e^-$. As a result, the depleted layer diminished, and the sensor resistances decreased accordingly. The sensor response increased with increased gas concentrations and working temperatures because of the increased adsorption and diffusion of C_2H_5OH gas on the surface and along the grain boundaries of the NFs. At the working temperature of 400˚C, the sensor response increased from 2.8 to 7.0 when the ethanol gas concentration increased from 100 to 1000 ppm. The gas sensing result to 100 ppm was quite similar to that of the sensor based on RGO loaded α-Fe_2O_3 composite prepared by hydrothermal method [25] and higher than that of the sensors based on pure α-Fe_2O_3 [27, 28]. The response time and recovery time of the sensor as a function of ethanol gas concentrations at the working temperature of 400˚C were shown in Fig. 3c. The response time of the sensor sharply decreased from 21s to 6s with increased gas concentrations from 100 ppm to 1000 ppm while the recovery time showed a reverse trend, from 72 s to 121 s. When C_2H_5OH gas concentrations increased from 100 to 1000 ppm, the time for the total adsorption of C_2H_5OH gas on the active sites of the NFs decreased, resulting in a reduction in the response time, whereas, the desorption time increased, leading to increased recovery time.

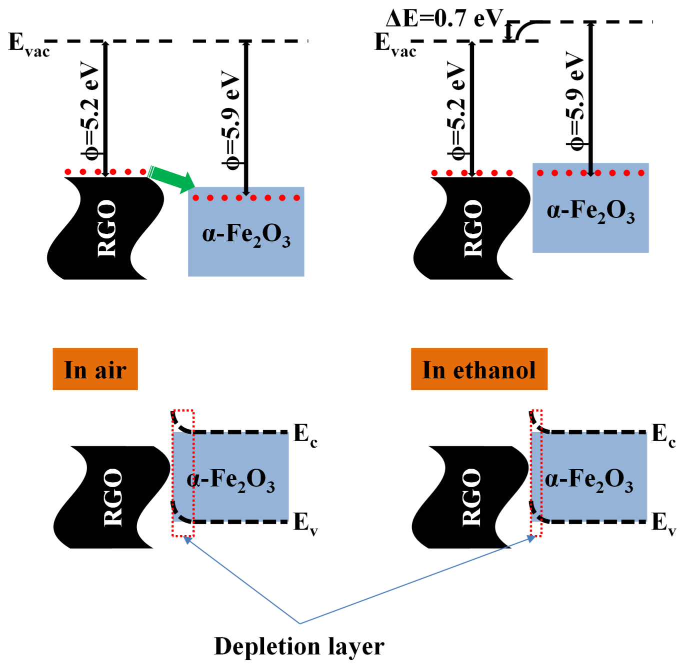

Fig. 4. Schematic ofH_2S sensing mechanisms of rGO/α-Fe_2O_3 NFs in the air, and in C_2H_5OH gas.

4. Conclusion

The RGO loaded α-Fe_2O_3 NFs were successfully prepared by the electrospinning method. The NFs with the rhombohedral crystal structure of the α-Fe_2O_3 matrix were 50-100 nm in diameter and consisted of many nanograins. The sensor based on RGO loaded α-Fe_2O_3 NFs showed a high response to ethanol gas. The sensor response increased when the ethanol gas concentrations and working temperatures increased. At the working temperature of 400°C, the sensor response, response time, and recovery time to 1000 ppm ethanol were approximately 7, 6 s, and 121 s, respectively.

Acknowledgments

This work was supported by the Vietnam National Foundation for Science and Technology Development (NAFOSTED) under grant number 103.02-2019.47.

Conflict of interest

The authors declare that they have no competing financial interests.

References

[1] G. Panthi, M. Park, H. Y. Kim, S. Y. Lee and S. J. Park, *Electrospun ZnO hybrid nanofibers for photodegradation of wastewater containing organic dyes: A review*, J. Ind. Eng. Chem. **21** (2015) 26.

[2] G. Panthi, M. Park, H. Y. Kim and S. J. Park, *Electrospun polymeric nanofibers encapsulated with nanostructured materials and their applications: A review*, J. Ind. Eng. Chem. **24** (2015) 1.

[3] M. J. Nalbandian, M. Zhang, J. Sanchez, Y.-H. Choa, J. Nam, D. M. Cwiertny and N. V. Myung, *Synthesis and optimization of Fe2O3 nanofibers for chromate adsorption from contaminated water sources*, Chemosphere **144** (2016) 975.

[4] S. Zhan, D. Chen, X. Jiao and S. Liu, *Facile fabrication of long α-Fe_2O_3, α-Fe and γ-Fe_2O_3 hollow fibers using sol–gel combined co-electrospinning technology*, J. Colloid and Interface Sci. **308** (2007) 265.

[5] S. Zolghadr, K. Khojier and S. Kimiagar, *Ammonia sensing properties of α-Fe_2O_3 thin films during post-annealing process*, Procedia Mater. Sci. **11** (2004) 469.

[6] A. Mirzaei, B. Hashemi and K. Janghorban, *α-Fe_2O_3 based nanomaterials as gas sensors*, J. Mater. Sci. Mater. Electron. **27** (2016) 3109.

[7] W. S. Hummers and R. E. Offeman, *Preparation of graphitic oxide*, J. Am. Chem. Soc. **80** (1958) 1339.

[8] S. Basu and P. Bhattacharyya, *Recent developments on graphene and graphene oxide based solid state gas sensors*, Sens. Actuators B. Chem. **173** (2012) 1.

[9] V. Singh, D. Joung, L. Zhai, S. Das, S. I. Khondaker and S. Seal, *Graphene based materials: Past, present and future*, Prog. Mater. Sci. **56** (2011) 1178.

[10] W. Yuan and G. Shi, *Graphene-based gas sensors*, J. Mater. Chem. A **35** (2013) 10078.

[11] L. Guo, X. Kou, M. Ding, C. Wang, L. Dong, H. Zhang, C. Feng, Y. Sun, Y. Gao, P. Sun and G. Lu, *Reduced graphene oxide/α-Fe_2O_3 composite nanofibers for application in gas sensors*, Sens. Actuators B Chem. 244 (2017) 233.

[12] S. Liang, H. Bi, J. Ding, J. Zhu, Q. Han and X. Wang, *Synthesis of α-Fe_2O_3 with the aid of graphene and its gas-sensing property to ethanol*, Ceram. Int. **41** (2015) 6978.

[13] T. Hu, X. Chu, F. Gao, Y. Dong, W. Sun and L. Bai, *Trimethylamine sensing properties of graphene quantum Dots/α-Fe_2O_3 composites*, J. Solid State Chem. **237** (2016) 284.

[14] H. Zhang, L. Yu, Q. Li, Y. Du and S. Ruan, *Reduced graphene oxide/α-Fe_2O_3 hybrid nanocomposites for room temperature NO_2 sensing*, Sens. Actuators B Chem. **241** (2017) 109.

[15] B. Zhang, Jie Liu, X. Cui, Y. Wang, Y. Gao, P. Sun, F. Liu, K. Shimanoe, N. Yamazoe and G. Lu, *Enhanced gas sensing properties to acetone vapor achieved by α-Fe_2O_3 particles ameliorated with reduced graphene oxide sheets*, Sens. Actuators B Chem. **241** (2017) 904.

[16] N. Van Hoang, P. H. Phuoc, C. M. Hung and N. Van Hieu, *The 12th Asian Conference on Chemical Sensors (ACCS2017)*, Hanoi (2017) 340–343.

[17] V. H. Nguyen, V. D. Nguyen, Q. D. Do, T. M. N. Quan, M. H. Chu and V. H. Nguyen, *On-chip ZnO nanofibers prepared by electrospinning method for NO_2 gas detection*, Comm. Phys. **27** (2018) 317.

[18] N. V. Hoang, C. M. Hung, N. D. Hoa, N. V. Duy and N. V. Hieu, *Facile on-chip electrospinning of ZnFe2O4 nanofiber sensors with excellent sensing performance to H_2S down ppb level*, J. Hazard. Mater. **360** (2018) 6.

[19] N. Van Hieu, N. D. Khoang, D. D. Trung, L. D. Toan, N. Van Duy and N. D. Hoa, *Comparative study on CO_2 and CO sensing performance of LaOCl-coated ZnO nanowires*, J. Hazard. Mater. **244–245** (2013) 209.

[20] N. V. Toan, N. V. Chien, N. V. Duy, H. S. Hong, H. Nguyen, N. D. Hoa and N. V. Hieu, *Fabrication of highly sensitive and selective H_2 gas sensor based on SnO_2 thin film sensitized with microsized Pd islands*, J. Hazard. Mater. **301** (2016) 433.

[21] D. D. Trung, N. Duc Hoa, P. V. Tong, N. V. Duy, T. D. Dao, H. V. Chung, T. Nagao and N. V. Hieu, *Effective decoration of Pd nanoparticles on the surface of SnO_2 nanowires for enhancement of CO gas-sensing performance*, J. Hazard. Mater. **265** (2014) 124.

[22] N. V. Hoang, C. M. Hung, N. D. Hoa, N. Van Duy, I. Park and N. V. Hieu, *Excellent detection of H_2S gas at ppb concentrations using ZnFe2O4 nanofibers loaded with reduced graphene oxide*, Sens. Actuators B Chem. **282** (2019) 876.

[23] N. V. Hoang, C. M. Hung, N. D. Hoa, N. V. Duy, N. V. Toan, H. S. Hong, P. T. H. Van, N. T. Son, S.-G. Yoon and N. V. Hieu, *Enhanced H_2S gas-sensing performance of α -Fe2O3 nanofibers by optimizing process conditions and loading with reduced graphene oxide*, J. Alloys Compd. **826** (2020) 1.

[24] Y. Cheng, H. Guo, Y. Wang, Y. Zhao,Y. Li, L. Liu, H. Li and H. Duan, *Low cost fabrication of highly sensitive ethanol sensor based on Pd-doped α-Fe_2O_3 porous nanotubes*, Mater. Res. Bull. **105** (2018) 21.

[25] L. Guo, X. Kou, M. Ding, C. Wang, L. Dong, H. Zhang, C. Feng, Y. Sun, Y. Gao, P. Sun, G. Lu, *Reduced graphene oxide/α-Fe_2O_3 composite nanofibers for application in gas sensors*, Sens. Actuators B Chem. **244** (2017) 233.

[26] L. Sun, J. Sun, K. Zhang, Xi Sun, S. Bai, Y. Zhao, R Luo, D. Li and A. Chen, *rGO functionalized α-Fe_2O_3/Co3O4 heterojunction for NO_2 detection*, Sens. Actuators B Chem. **354** (2022) 131194.

[27] W. Zheng, Z. Li, H. Zhang, W. Wang, Y. Wang, and C. Wang, *Electrospinning route for α-Fe_2O_3 ceramic nanofibers and their gas sensing properties*, Mater. Res. Bull. **44** (2009) 1432.

[28] C. M. Hung, N. D. Hoa, N. V. Duy, N. V. Toan, D. T. T. Le and N. V. Hieu, *Synthesis and gas-sensing characteristics of α-Fe_2O_3 hollow balls*, J. Sci. Adv. Mater. Devices **1** (2016) 45.